Soft Matter

PAPER

View Article Online
View Journal | View Issue

Cite this: *Soft Matter*, 2021, 17, 5763

The effect of headgroup methylation on polymorphic phase behaviour in hydrated *N*-methylated phosphoethanolamine:palmitic acid membranes†

Matthew E. Allen, [a] Yuval Elani, [b] Nicholas J. Brooks [a] and John M. Seddon *[a]

Received 2nd February 2021,
Accepted 14th May 2021

DOI: 10.1039/d1sm00178g

rsc.li/soft-matter-journal

Mixtures of fatty acids and phospholipids can form hexagonal (H_{II}) and inverse bicontinuous cubic phases, the latter of which are implicated in various cellular processes and have wide-ranging biotechnological applications in protein crystallisation and drug delivery systems. Therefore, it is vitally important to understand the formation conditions of inverse bicontinuous cubic phases and how their properties can be tuned. We have used differential scanning calorimetry and synchrotron-based small angle and wide angle X-ray scattering (SAXS/WAXS) to investigate the polymorphic phase behaviour of palmitic acid/partially-methylated phospholipid mixtures, and how headgroup methylation impacts on inverse bicontinuous cubic phase formation. We find that upon partial methylation of the phospholipid headgroup (1 or 2 methyl substituents) inverse bicontinuous cubic phases are formed (of the *Im3m* spacegroup), which is not the case with 0 or 3 methyl substituents. This shows how important headgroup methylation is for controlling phase behaviour and how a change in headgroup methylation can be used to controllably tune various inverse bicontinuous phase features such as their lattice parameter and the temperature range of their stability.

Introduction

Lipids and other amphiphilic molecules can self-assemble to form a wide variety of liquid-crystalline phases[1] depending on their chemical structure and interaction properties. Amphiphilic molecules can be broadly classified into 3 types (type 0, I or II amphiphiles). Type 0 amphiphiles are bilayer forming as the headgroup and the hydrocarbon tail exert similar lateral pressures. On the other hand, type I or II amphiphiles are non-bilayer forming as the headgroup and hydrocarbon tail exert different lateral pressures, thus leading to a tendency for the polar/nonpolar interface to curve either towards the tail or headgroup regions respectively.[2]

Due to the different self-assembly properties of amphiphiles, structures that include crystalline, gel and fluid lamellar phases (L_C, L_β and L_α respectively) and non-lamellar phases can be formed from bilayer forming and non-bilayer forming amphiphiles respectively (Fig. 1). Particularly important non-lamellar phases include the inverse hexagonal phase (H_{II}) where the lipids are arranged into inverse cylinders, with water on the inside, that pack onto a 2-D hexagonal lattice,[3] and inverse bicontinuous cubic phases (Q_{II}^D, Q_{II}^G, Q_{II}^P), where a continuous lipid bilayer is draped onto a D, G or P infinite minimal periodic surface, giving rise to cubic phases of *Pn3m*, *Ia3d* and *Im3m* crystallographic space groups respectively.[4]

Non-lamellar phases, due to their interfacial curvature, are important *in vivo* as they have important biological functions[5] and affect biological membrane organisation.[6] Inverse bicontinuous cubic phases are known to appear within mammalian cells[7,8] and are associated and formed within cells that have experienced stress,[9] starvation[10] and infection by viruses.[11]

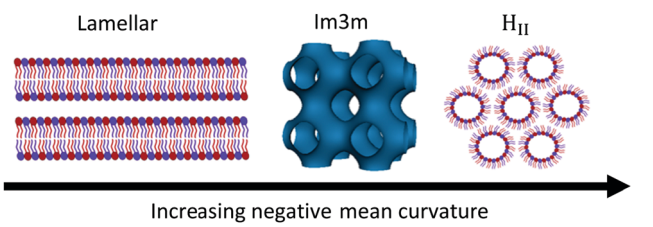

Fig. 1 Schematic of the lamellar phase, an inverse bicontinuous cubic phase (*Im3m* spacegroup) and the inverse hexagonal phase and how they are related by interfacial curvature.

[a] *Department of Chemistry, Imperial College London, W12 7SL, UK. E-mail: j.seddon@imperial.ac.uk*
[b] *Department of Chemical Engineering, Imperial College London, SW7 2AZ, UK*

† Electronic supplementary information (ESI) available. See DOI: 10.1039/d1sm00178g

For example the SARS coronavirus causes formation of a *Ia3d* gyroid phase[12] within cells infected by this virus.[13]

In vitro inverse bicontinuous cubic phases have attracted significant attention due to their unique properties;[14] they are soft biocompatible structures that have a large surface area due to their interconnected water pore network. Therefore, inverse bicontinuous cubic structures have found uses as drug delivery platforms[15,16] and protein crystallisation systems[17,18] where amphiphile composition,[19] stereochemical purity,[20] water content,[21] charge of the system,[22] solvents,[23] pH,[24] pressure and temperature[25] can be altered to achieve a particular bicontinuous cubic spacegroup or bicontinuous cubic lattice parameter.

A particularly interesting set of biological amphiphiles that can induce inverse bicontinuous cubic structures are long chain fatty acids. These molecules have been observed to be important in membrane fusion events[26,27] and can influence biological functions by regulating ion channel activity,[28] membrane fluidity[29] and bending rigidity[30] in addition to affecting cell signalling behaviour.[31] Specifically oleic acid can reduce blood pressure through controlling G-protein mediated signalling by promoting inverse hexagonal phase behaviour at high contents.[32] Additionally, palmitic acid, the most common saturated fatty acid in the body[33] can impair insulin signalling and increase hepatocyte apoptosis.[34] Therefore, it is critically important to gain an understanding of how lipids and fatty acids combine to influence membrane phase behaviour and function. This will enable exploitation of these mixtures properties to design biologically relevant and useful inverse bicontinuous cubic systems.

Previous work has looked at how saturated fatty acid composition affects the phase behaviour of the natural bilayer forming phosphatidylcholine (PC) phospholipids.[35] It was observed that the incorporation of fatty acids shifts the gel–fluid transition to higher temperatures[36] and at significant molar fatty acid fractions (0.67 mol fraction) the L_β–L_α gel–fluid transition present in pure phosphatidylcholine systems shifts towards a L_β–H_{II} transition.[37] Thus, the fluid bilayer L_α phase is completely suppressed, due to the fatty acid affecting the membrane lateral pressure profile. This leads to the favouring of non-lamellar phase formation.[38,39] Furthermore, at this stoichiometry sharp phase transitions occur due to formation of a 2 : 1 fatty acid : phospholipid complex, and azeotropic behaviour is observed at this point.[40] Moreover for short chain fatty acid:phosphatidylcholine mixtures (lauric acid:DLPC and myristic acid:DMPC) inverse bicontinuous cubic phase formation is exhibited at the 2 : 1 fatty acid : phospholipid ratio.[21] However, at longer chain lengths (palmitic acid:DPPC) there is no evidence of inverse bicontinuous cubic phase formation for this composition.

As headgroup methylation impacts the uptake of important biological molecules such as L-arginine[41] and affects cell signalling pathways,[42] the influence of headgroup methylation within membranes is an important topic to explore. Phosphatidylethanolamines (PE), phospholipids that have no headgroup methylation, and readily form non-lamellar phases such as H_{II} and bicontinuous cubic phases at elevated temperatures,[43,44] have a more significant non-bilayer forming characteristic than PC phospholipids. Furthermore,

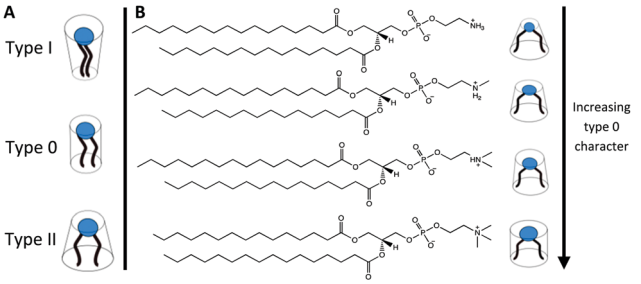

Fig. 2 (A) Schematic of the typical lipid types based on their tendency for the polar/nonpolar interface to curve either towards the tail (type I), neither (type 0) or the headgroup (type II). (B) The chemical structures of (from top to bottom) DPPE, DPPE-me, DPPE-me_2, and DPPC with schematics indicating the type of the amphiphile.

phospholipids with a partially methylated headgroup structure, *i.e.* one or two methylations of the headgroup nitrogen (Fig. 2) also exhibit different phase behaviour to that of PC or PE phospholipids[45–47] and have bilayer forming tendencies that are in between those of PC and PE phospholipids. In particular single *N*-methylated DOPE (DOPE-me) shows inverse bicontinuous cubic and H_{II} phase formation.[48,49] Therefore, by altering the hydrogen bonding network and the headgroup size (spontaneous radius of curvature[50]) through changing the nitrogen methylation of the phospholipid headgroup, inverse bicontinuous cubic phase formation can be suppressed or encouraged.

In this work we have investigated how palmitic acid (PA) interacts with 1,2-dipalmitoyl-*sn-glycero*-3-phosphoethanolamine-*N*-methyl (DPPE-me) and 1,2-dipalmitoyl-*sn-glycero*-3-phosphoethanolamine-*N*,*N*-dimethyl (DPPE-me_2) phospholipids. These phospholipids along with DPPE and DPPC ordinarily show gel–fluid lamellar transitions between 40 and 70 °C.[46] We have seen that by altering the headgroup methylation that inverse bicontinuous cubic phases can be formed in these longer chain fatty acid:phospholipids mixtures. Moreover 2 : 1 palmitic acid : phospholipid samples were analysed across a range of headgroup methylations (DPPE, DPPE-me, DPPE-me_2 and DPPC) to rationalise the effect of headgroup methylation on phase behaviour. Demonstrating that these essential biological molecules can form inverse bicontinuous cubic phases and properties such as phase formation temperature and lattice parameters can be adjusted by headgroup methylation allows exploitation of this knowledge to design new biologically and therapeutically important systems. Furthermore, the rationale behind the impact of headgroup methylation within these systems can be applied to existing formulations[51] to further enhance their potential use.

Experimental

Materials

The phospholipids DPPE (1,2-dipalmitoyl-*sn-glycero*-3-phosphoethanolamine), DPPE-me (1,2-dipalmitoyl-*sn-glycero*-3-phospho ethanolamine-*N*-methyl), DPPE-me_2 (1,2-dipalmitoyl-*sn-glycero*-3-phosphoethanolamine-*N*,*N*-dimethyl) and DPPC (1,2-dipalmitoyl-*sn-glycero*-3-phosphocholine) were purchased from Sigma Aldrich

(Gillingham, UK) as powders. Palmitic acid was also purchased from Sigma Aldrich (Gillingham, UK) as a powder. All of the chemicals had a purity of >99% and were used without subsequent purification.

Sample preparation

Samples were prepared by co-dissolving appropriate amounts of the phospholipid and palmitic acid in chloroform (Sigma Aldrich, Gillingham, UK). The solutions were then vortexed to ensure mixing before the chloroform was removed under a stream of N_2 gas. The resultant films were lyophilised for at least 12 hours before being hydrated with ultrapure water (18.2 mΩ) to a 70% water weight fraction in order to ensure the samples were under excess hydration conditions.

DSC preparation and measurements

A known weight of the hydrated phospholipid:palmitic acid mixture was placed into a hermetically sealed DSC pan. A PerkinElmer Diamond DSC was then used to analyse the samples; before any data were recorded the samples underwent at least 2 heating/cooling cycles on the DSC to ensure homogenous mixing without any water loss. A scan rate of 1 °C was used to obtain thermographs of the samples from which the transition temperatures and phase transition behaviour were obtained.

X-Ray preparation and measurements

The hydrated phospholipid:palmitic acid samples were placed into 1.8 mm inner diameter polycarbonate capillaries that were sealed with epoxy resin. The sealed capillaries were heat cycled to ensure homogenous mixing while minimising water loss. Small and wide-angle X-ray diffraction data were obtained for the mixed samples using beamline I22 at Diamond Light Source. Diffraction patterns were collected using an X-ray energy of 18 keV (wavelength 0.689 Å) and a sample to detector distance of 2 m. The raw data were corrected using the procedure developed by the beamline technicians at Diamond.[52] The processed data were analysed by fitting pseudo-Voigt functions to Bragg peaks in order to extract peak maxima values that were used to calculate the *d*-spacings, and hence the lattice parameters once the lipid mesophases had been correctly identified from indexing of the Bragg peaks (see ESI,† Fig. S6 or S10 for more detail).

Results and discussion

The phase behaviour of DPPE-me:palmitic acid complexes

Initially DSC and X-ray diffraction experiments were used to characterise the phase behaviour of PA:DPPE-me mixtures in excess water. The experimental results are summarised in Fig. 3. At low molar concentrations of palmitic acid (0.33 mol fraction) the phases identified through SAXS (the L_β and L_α phases) were the same as those seen within pure DPPE-me. This matches previous observations in PA:DPPC samples where small amounts of palmitic acid did not alter the phase behaviour.[39] However, upon adding a significant amount of palmitic acid (0.5 mol fraction) a H_{II} phase was seen instead of the L_α phase. This occurs as palmitic acid is a non-bilayer forming amphiphile,[53] hence at a high enough concentration of palmitic acid the phase behaviour shifts to favour non-lamellar structures to reduce the increased curvature

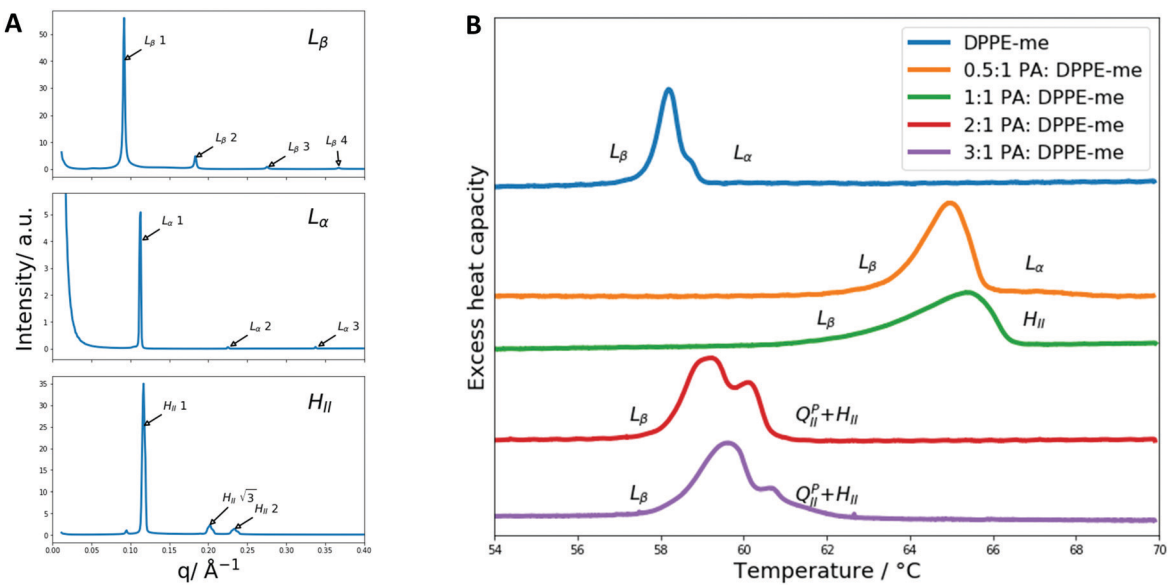

Fig. 3 Identification of the phases and phase transitions present in PA:DPPE-me mixtures. (A) Representative SAXS patterns of the 3 main non cubic phases encountered during this work where the main phase peaks of interest are indexed. The L_β pattern is from the 0.5 : 1 PA : DPPE-me composition at 50 °C, the L_α pattern was obtained from the 0.5 : 1 PA : DPPE-me composition at 65 °C and the H_{II} pattern was measured from the 1 : 1 PA : DPPE-me composition at 65 °C. (B) DSC thermographs of PA:DPPE-me mixtures at different stoichiometries, and pure DPPE-me, with their respective phase transitions indicated.

frustration energy within the phospholipid bilayer.[54] Through using DSC, the addition of palmitic acid led to a broadening and increase in the transition temperature of the gel–fluid phase transition peak. This again has been observed within PA:DPPC samples.[39] DSC also verified that at higher palmitic acid concentrations (0.5 mol fraction) the main gel–fluid phase transition occurred between the L_β and H_{II} phases.

However, the molar fraction of palmitic acid needed to induce the L_β–H_{II} transition is lower than the amount reported in PA:DPPC mixtures. This occurs as DPPE-me has a smaller headgroup than DPPC and thus has a larger degree of non-bilayer forming character (characterised by a smaller spontaneous radius of curvature[50]). This allows the H_{II} phase to be formed more readily.

At higher concentrations of palmitic acid (0.67 and 0.75 mol fractions), the gel–fluid transition still corresponds to L_β–H_{II}, although the transition temperature has decreased significantly. This arises from the increased presence of non-bilayer forming amphiphiles increasing the curvature frustration energy within the bilayer thus favouring the formation of the H_{II} phase at a lower temperature.

The phase transition peak for the 2 : 1 ratio of palmitic acid : DPPE-me is sharper than the 3 : 1 ratio, because the azeotropic point of PA : DPPE-me occurs at the former composition. This matches previous work where FA:PC mixtures exhibit a sharp DSC transition and an azeotropic point at this molar ratio.[35] This further enhances the argument that PA : DPPE-me mixtures also experience the formation of a 2 : 1 complex and shows the 2 : 1 fatty acid : phospholipid complex formation is common among phospholipid : fatty acid mixtures.

Furthermore, at high concentrations of palmitic acid (0.67 and 0.75 mol fractions) a double humped transition is present indicating that more complex phase behaviour is occurring than what was present with lower palmitic acid concentrations and 2 : 1 palmitic acid : DPPC mixtures. As a result, we collected SAXS and WAXS measurements at temperatures from 54 to 65 °C to investigate the phase behaviour more closely. The data are summarised in Fig. 4.

Once again, the SAXS and WAXS spectra demonstrate the main phase change occurring is a L_β–H_{II} transition shown by the 1, 2, 3, 4 reflections at 54 °C for the L_β phase and the 1, $\sqrt{3}$, 2, $\sqrt{7}$ reflections at 65 °C for the H_{II} phase. This transition was also accompanied by an increase in fluidity shown by the broadening of the sharp peak in the WAXS spectra. Furthermore, at lower temperatures a peak at 0.175 $Å^{-1}$ that matched crystalline palmitic acid (ESI,† Fig. S4) was present. This indicates that 'excess' palmitic acid crystallises out of the membrane and forms its own crystalline phase at high molar fractions (demonstrated within ESI,† Fig. S5) which matches previous observations.[39] At higher temperatures the palmitic acid peaks disappear which is indicative of palmitic acid melting into an isotropic liquid.

From the onset of the gel–fluid transition (59 °C) to 65 °C another set of peaks appear alongside the H_{II} phase peaks. These peaks have been assigned the *Im3m* cubic space group

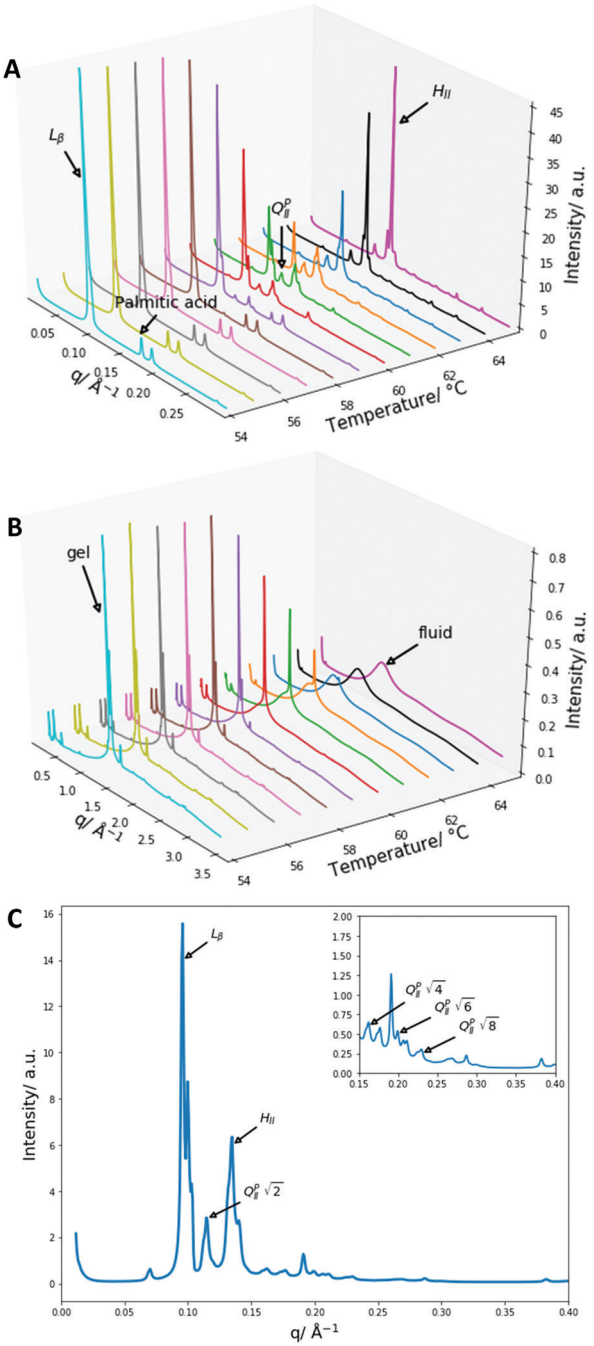

Fig. 4 X-Ray diffraction data of 2 : 1 PA : DPPE-me mixtures (A) SAXS patterns from 54 to 65 °C with an identification of the main liquid-crystalline phase peaks and the palmitic acid precipitate. (B) WAXS patterns from 54 to 65 °C with an indication of the gel and fluid phases. (C) The SAXS diffraction pattern at 61 °C, the first peaks of the main liquid crystalline phases and all of the Q^P_{II} phase peaks are identified, the inserted smaller graph enlarges the peaks in the region from 0.15 to 0.4 $Å^{-1}$.

(Q^P_{II}), with the first 4 reflections $\sqrt{2}$, $\sqrt{4}$, $\sqrt{6}$, $\sqrt{8}$ present and indicated (Fig. 4C). Furthermore, earlier studies looking at inverse bicontinuous cubic phase formation in the shorter chain 2 : 1 myristic acid : DMPC mixtures gave evidence of H_{II} and Q^P_{II} coexistence[21] at excess water weight fractions. As this

system is very similar to the system being investigated this gives additional weighting to the *Im3m* assignment.

Other unassigned peaks indicate other structures are present in the mixture. However, these peaks cannot be assigned unambiguously due to the lack of reflections present. The weak yet prominent peak present at 0.070 $Å^{-1}$ does not align with any of the already assigned peaks or agree with theoretical Bonnet ratios[55]that would have indicated another inverse bicontinuous cubic phase was present alongside the already assigned *Im3m* phase.

The *Im3m* inverse bicontinuous cubic phase identified has a lattice parameter of 77.08 Å (ESI,† Fig. S6) at 61 °C which is small when compared to *Im3m* lattice parameters in other fatty acid:phospholipid mixtures.[21,53] This is rationalised by DPPE-me containing more non-bilayer forming character than PC phospholipids thus leading to a more curved *Im3m* phase with a smaller lattice parameter.

The coexistence between the Q_{II}^{P} and H_{II} phases is explained by their formation occurring through a common intermediate. Upon a lamellar to non-lamellar phase transition, the lamellar phase bilayers form trans monolayer contacts.[56] This structure can then produce the H_{II} phase through a series of precursor structures or inverse bicontinuous cubic phases if enough interlamellar attachments are formed.[57] Partially methylated phosphatidylethanolamines (DPPE-me) have been shown to form interlamellar attachments around phase transition temperatures[49] while phosphatidylcholines (DPPC) do not form such interlamellar attachments due to their large spontaneous radius of curvature.[45] This results in Q_{II} phase formation within PA:DPPE-me systems but not in PA:DPPC systems.[35]

More recently the formation of interlamellar attachments has been linked to the Gaussian curvature elastic modulus of monolayers.[58] This value is dependent on the amphiphile composition, hence Q_{II} phase formation will be dependent on the molar concentration of palmitic acid hereby explaining Q_{II}^{P} phase formation occurring only at the 2:1 and 3:1 PA:DPPE-me stoichiometries.

The phase behaviour of DPPE-me_2:palmitic acid mixtures

Next, we explored the impact of one additional headgroup methyl group. Thus, PA:DPPE-me_2 mixtures in excess water had their phase behaviour characterised through DSC and X-ray diffraction experiments. The results from these experiments are summarised in Fig. 5.

Once again through SAXS the L_α phases seen within pure DPPE-me_2 were replaced with H_{II} phases upon addition of palmitic acid. Moreover, using DSC, palmitic acid addition again broadened the phase transitions; however, the gel–fluid transition temperature increase was more significant than with DPPE-me. Furthermore, the onset of the L_β–H_{II} phase transition occurred at a lower molar palmitic acid content (0.33 mol fraction) than for PA:DPPE-me and PA:DPPC.[39] Therefore, palmitic acid is again inducing the formation of non-lamellar phases, although the earlier onset of this transition compared to the more intrinsically curved PA:DPPE-me mixtures[45] that contain a smaller headgroup (DPPE-me)

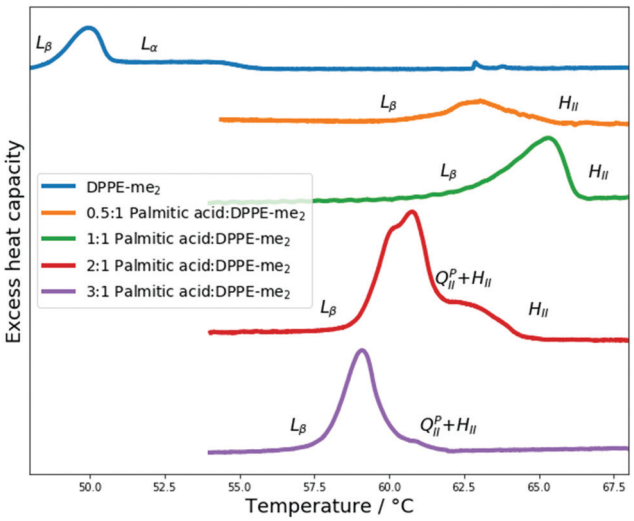

Fig. 5 DSC scans of PA:DPPE-me_2 mixtures and pure DPPE-me_2, with their respective phase transitions indicated.

indicates that the induction of the H_{II} phase is more complex than just increasing the spontaneous curvature in the complex.

Another parameter affecting H_{II} phase formation is hydrogen bonding between the headgroups within the lipid membrane and the surrounding water. Upon increased headgroup methylation of the phospholipid headgroup the ability to interact with neighbouring headgroups and both the external water through hydrogen bonding decreases due to the sequential loss of first one, then two hydrogen atoms which act as hydrogen bond donors.[59] Hence within PA:phospholipid mixtures changing the methylation of the headgroup and increasing the amount of palmitic acid both affect the hydrogen bonding network of the mixture. Within PA:DPPE-me mixtures increasing the palmitic acid content reduces hydrogen bonding through reducing the number of H bond donors, this has been argued to alter the intermolecular forces within the bilayer and between bilayers.[60] This leads to an increase in the area per molecule within the bilayer[61] and thus increases the spontaneous radius of curvature which leads to the disfavouring of H_{II} phases. However, in PA:DPPE-me_2 mixtures palmitic acid addition alters the hydrogen bonding network very little leading to no phase formation favouring/disfavouring due to hydrogen bonding. The above potentially rationalises why PA:DPPE-me_2 forms H_{II} phases at a lower palmitic acid content than PA:DPPE-me. Furthermore, within PA:DPPC mixtures hydrogen bonding is increased upon palmitic acid addition due to the availability of more hydrogen bonding donors. Using the same argument as above the spontaneous radius of curvature will be decreased favouring the formation of the H_{II} phase. This also further rationalises why DPPC, a bilayer forming phospholipids, can form non-lamellar phases when mixed with fatty acids.

At higher palmitic acid concentrations (0.67 and 0.75 mol fractions) a decrease in the L_β–H_{II} transition temperature is once again seen. This matches observations in PA:DPPE-me bilayers (Fig. 3) that the significantly increased presence of palmitic acid increases the curvature frustration energy and

favours lower temperature H_{II} phase formation. As before, the phase transitions around the 0.67 mol fraction are more distinct and sharper giving further credence to the idea that fatty acids and phospholipids form 2 : 1 complexes[35] and that this complex formation is not limited to PC based phospholipids.

The 2 : 1 PA : DPPE-me_2 mixture also exhibits a double humped transition. To verify that inverse bicontinuous cubic phase formation was again behind this complex phase behaviour SAXS and WAXS measurements were collected between 54 and 65 °C. The data are summarised in Fig. 6.

Once more, as with 2 : 1 PA : DPPE-me the main transition occurring is the L_β–H_{II} transition shown by the presence of the 1, 2, 3, 4 reflections at 54 °C for the L_β phase and the 1, $\sqrt{3}$, 2 reflections at 65 °C for the H_{II} phase. The gel peak in the WAXS spectra once again broadened at the phase transition temperature confirming that a gel–fluid transition was occurring. The peak at 0.175 $Å^{-1}$ again matched crystalline palmitic acid (ESI,† Fig. S4) and matches previous work shown within this paper and other papers[39] on the phase separation of palmitic acid from the membrane at high molar contents, giving further weight to the idea that this occurs across a range of different membranes.

At the onset of the gel–fluid transition (60 °C) a set of peaks coexist with the H_{II} phase peaks over a very narrow temperature range (59–62 °C). Again, some of these peaks can be assigned to the *Im3m* inverse bicontinuous cubic space group (Q^P_{II}) with the first 3 reflections $\sqrt{2}$, $\sqrt{4}$, $\sqrt{6}$ (which is very faint) present and indicated in Fig. 4C. As this system is very similar to the better characterised *Im3m* phase in the 2 : 1 PA : DPPE-me system and previous systems that showed *Im3m* phases at excess water,[21] the *Im3m* phase can be assigned.

As with 2 : 1 PA : DPPE-me, in PA : DPPE-me_2 mixtures there are unassigned peaks present which cannot be assigned unambiguously due to the lack of reflections present or agreement with theoretical Bonnet ratios.[55] However, these unassigned peaks appear in the same regions of the PA:DPPE-me and PA:DPPE-me_2 patterns and at similar positions in relation to the Q^P_{II} reflections. The appearance of these peaks in the same positions across a range of headgroup methylations suggests that the peaks are related in some way to non-lamellar phase formation.

The lattice parameter of the *Im3m* inverse bicontinuous cubic phase was 86.0 Å at 62 °C (ESI,† Fig. S10), this value is significantly larger than the lattice parameter values of 2 : 1 PA : DPPE-me at 61 and 62 °C (77.1 and 74.1 Å respectively) indicating that the larger lattice parameter occurs due to DPPE-me_2 having a larger headgroup than DPPE-me thus leading to a less curved *Im3m* phase.

The ratio of the *Im3m* : H_{II} peak intensities within the 2 : 1 PA : DPPE-me_2 sample is smaller than the same ratio within the 2 : 1 PA : DPPE-me sample. This indicates that along with the small range of *Im3m* stability in the 2 : 1 PA : DPPE-me_2 sample, that the H_{II} phase is increasingly favoured over the *Im3m* phase upon increasing headgroup methylation at this stoichiometry. This follows previous rationale suggesting that DPPE-me_2, due to its larger headgroup, will have a larger spontaneous radius of curvature, thus forming fewer interlamellar attachments during the lamellar–non lamellar transition.[45] This will reduce the prevalence of the Q_{II} phases as seen in the SAXS data. Furthermore, the stability of the Q_{II} phases is related to the temperature dependent Gaussian curvature elastic modulus,[58] thus an increase in temperature leads to a change in this value which causes the destabilisation of the Q_{II} phases and favouring of the H_{II} phase.

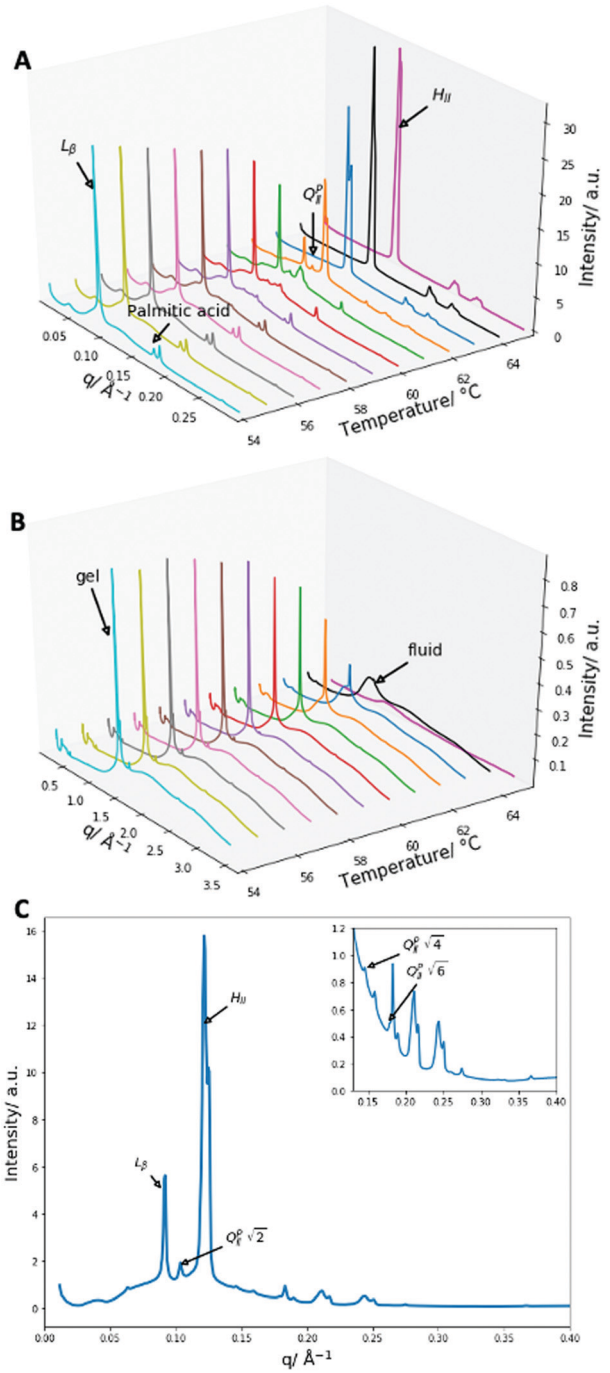

Fig. 6 X-Ray diffraction data of 2 : 1 PA : DPPE-me_2 mixtures (A) SAXS patterns from 54 to 65 °C with an identification of the main liquid-crystalline phase peaks and the excess palmitic acid precipitate. (B) WAXS patterns from 54 to 65 °C with an indication of the gel and fluid phases. (C) The SAXS diffraction pattern at 62 °C, the first peaks of the main liquid crystalline phases and all of the Q^P_{II} phase peaks are identified, and the inserted smaller graph enlarges the peaks in the region from 0.14 to 0.4 $Å^{-1}$.

With other stoichiometries of PA:DPPE-me$_2$ *Im3m* space-groups are also present. Evidence for this is again seen in the 3 : 1 mixture, which despite a single melting peak in the DSC scan exhibits remarkably similar phase behaviour to the 2 : 1 PA : DPPE-me$_2$ sample. However, one key difference is the stability of the Q_{II}^{P} phase, in the 3 : 1 sample the Q_{II}^{P} phase is stable across a wider temperature range (ESI,† Fig. S7) potentially indicating that the slightly increased concentration of palmitic acid helps stabilise this phase relative to the H_{II} phase. Furthermore, within the 1 : 1 stoichiometry there are two unassigned peaks at high temperatures that correlate to $\sqrt{2}$ and $\sqrt{4}$ *Im3m* reflections (ESI,† Fig. S8) although lack of any further peaks means that an assignment cannot be completed with confidence. More work needs to be done to further identify the region of Q_{II} phase formation in both PA:DPPE-me and PA:DPPE-me$_2$ systems.

The effect of headgroup methylation on phase behaviour

After characterising the phase behaviour of PA:DPPE-me and PA:DPPE-me$_2$ mixtures and gaining an understanding of what factors affect inverse bicontinuous cubic phase formation in these samples, we investigated the effect of headgroup methylation across the 2 : 1 PA : phospholipid mixtures and in the pure phospholipid samples in excess water. This was done in order to further understand how both lamellar and non-lamellar phase behaviour is affected by the degree of methylation. The results from this are summarised in Fig. 7.

For the pure phospholipid samples an increase in headgroup methylation decreases the L_β–L_α transition temperature (or in the case of DPPC the ripple gel P_β'–L_α transition temperature), a trend that has been observed by others.[46] This is in part due to the decrease in hydrogen bonding promoting lateral expansion within the bilayer leading to a lower temperature where the bilayer fluidises.[62]

Conversely, for the 2 : 1 samples, an increase in phospholipid headgroup methylation increases the transition temperature. As the transitions are all lamellar–non lamellar, a different set of energetics govern these transitions when compared to the pure phospholipids. As discussed previously an increase in headgroup methylation increases the spontaneous radius of curvature of the phospholipids. As a larger spontaneous radius of curvature disfavours H_{II} phase formation,[45] a higher L_β–H_{II} transition temperature will be seen for the larger headgroup phospholipids. In addition, increasing headgroup methylation will decrease hydrogen bonding and thus alter the intermolecular forces within and between bilayers.[60] As discussed before this leads to an increase in the area per molecule within the bilayer,[61] increasing the spontaneous radius of curvature, and disfavouring H_{II} phase formation. The 2 : 1 samples also clearly show that Q_{II}^{P} phase formation is favoured at intermediate degrees of methylation which supports previous work in the field.[45,58]

When comparing the pure phospholipid samples to the 2 : 1 mixture samples it is clear that headgroup methylation influences phospholipid phase behaviour in greatly different ways depending on the transition involved. This shows a simple change to phospholipid structure can lead to complex changes of self-assembly properties of the system.

In addition to investigating the effects of headgroup methylation on phase behaviour, the effects of headgroup methylation on the *d* spacings of the L_β phase at 50 °C and the H_{II} phase at 65 °C in 2 : 1 PA : phospholipid samples were analysed. The results are summarised in Fig. 8.

Throughout both the phases an increase in methylation increases the *d* spacing values. However, within the L_β phase consecutive increases in methylation have less effect on the *d* spacing values while within the H_{II} phase the increase is more linear.

For the L_β phase an initial large increase upon methylation is attributed to a single methyl group having a greater degree of steric interference compared to a hydrogen atom. This interferes with the ability of the headgroup to interact with other headgroups between bilayers,[63] which will increase the *d* spacing. Due to long axis rotation within the bilayers, subsequent methylation will impact the ability of the phospholipids to hydrogen bond far more than affect the sterics of the system. In addition DPPC has been seen to tilt to fill in void space within the hydrocarbon tail region[64] and reduce the steric impact of having a large headgroup. Therefore, the slight increases after the initial methylation are due to a reduction in interactions

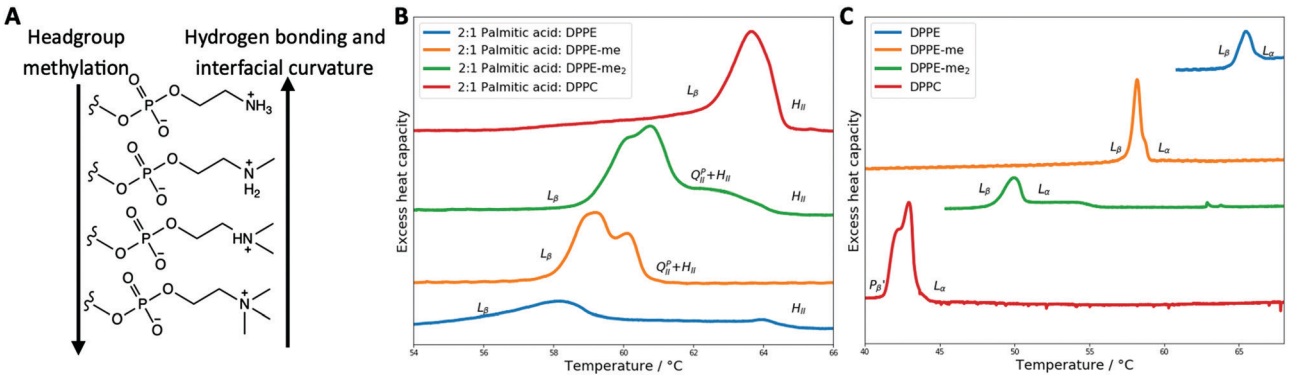

Fig. 7 The impact of headgroup methylation on phase behaviour and transition temperatures. (A) Schematic presenting how phospholipid headgroup methylation impacts on hydrogen bonding and preferred interfacial curvature. (B) DSC thermograph showing the effects of headgroup methylation in 2 : 1 palmitic acid : phospholipid mixtures. (C) DSC thermograph showing the effects of headgroup methylation in pure phospholipid systems.

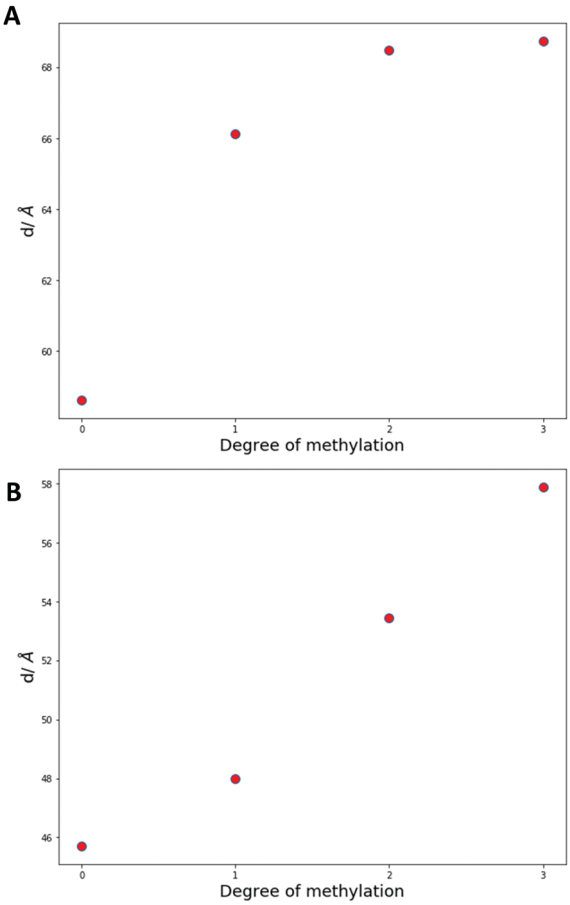

Fig. 8 Effect of headgroup methylation on *d* spacings in 2 : 1 palmitic acid : phospholipid mixtures. (A) *d* spacing values of the L_β phase at 50 °C. (B) *d* spacing values of the H_{II} phase at 65 °C. The error bars are approximately the size of the plotted data points.

between bilayers predominantly caused by hydrogen bonding. These results for the L_β phase align closely with results for pure phospholipid systems where a large increase in *d* spacing was evident upon the initial methylation and subsequent methylations led to little change in this parameter.[45]

In the more fluid H_{II} phase, due to the larger volume available for the molecules to occupy, the effect of sterics on screening interactions between molecules is reduced significantly. Thus, the increase in *d* spacing upon methylation can be attributed to decreasing interaction strengths predominantly through hydrogen bonding between molecules. This fits with the largely linear data that suggests a near constant change in forces is occurring to increase the *d* spacing. Increasing methylation removes one hydrogen bonding equivalent which would lead to a similar change in forces upon each methylation.

Conclusions

In this study we have demonstrated that inverse bicontinuous cubic phases of spacegroup *Im3m* can be formed in palmitic acid:phospholipid mixtures by altering the headgroup methylation. We also showed both palmitic acid content and the methylation of the phospholipid headgroup play vital roles in phase formation. Furthermore, the impact of phospholipid methylation within fatty acid systems has been shown to impact on *d*-spacings as well as phase formation. Showing that longer chain saturated fatty acids systems can form inverse bicontinuous cubic phases and how headgroup methylation affects these systems will hopefully enable the production of biological system mimics involving these components. In addition, the increased understanding of the effect of headgroup methylation will improve our ability to tune inverse bicontinuous cubic systems and further enhance uses in different fields such as drug delivery and protein crystallisation.

Conflicts of interest

There are no conflicts to declare.

Acknowledgements

We acknowledge Diamond Light Source for time on beamline I22 under proposal SM20789 and would like to thank Dr Andy Smith for his support and assistance in using the beamline. This work was supported by EPSRC Programme grant EP/J017566/1 and a UKRI Future Leaders Fellowship, grant reference number MR/S031537/1.

Notes and references

1 V. Luzzati and F. Husson, *J. Cell Biol.*, 1962, **12**, 207–219.
2 G. C. Shearman, O. Ces, R. H. Templer and J. M. Seddon, *J. Phys.: Condens. Matter*, 2006, **18**, S1105–S1124.
3 J. M. Seddon, *Biochim. Biophys. Acta, Biomembr.*, 1990, **1031**, 1–69.
4 G. C. Shearman, A. I. I. Tyler, N. J. Brooks, R. H. Templer, O. Ces, R. V. Law and J. M. Seddon, *Liq. Cryst.*, 2010, **37**, 679–694.
5 O. Vögler, J. Casas, D. Capó, T. Nagy, G. Borchert, G. Martorell and P. V. Escribá, *J. Biol. Chem.*, 2004, **279**, 36540–36545.
6 J. Jouhet, *Front. Plant Sci.*, 2013, 4.
7 T. Landh, *FEBS Lett.*, 1995, **369**, 13–17.
8 Z. A. Almsherqi, S. D. Kohlwein and Y. Deng, *J. Cell Biol.*, 2006, **173**, 839–844.
9 Y. Deng and Z. A. Almsherqi, *Interface Focus*, 2015, 5.
10 E. W. Daniels and E. P. Breyer, *Zeitschrift für Zellforsch. und Mikroskopische Anat.*, 1968, **91**, 159–169.
11 Y. Deng, Z. A. Almsherqi, M. M. L. Ng and S. D. Kohlwein, *Trends Cell Biol.*, 2010, **20**, 371–379.
12 Z. A. Almsherqi, C. S. McLachlan, P. Mossop, K. Knoops and Y. Deng, *Redox Rep.*, 2005, **10**, 167–171.
13 C. S. Goldsmith, K. M. Tatti, T. G. Ksiazek, P. E. Rollin, J. A. Comer, W. W. Lee, P. A. Rota, B. Bankamp, W. J. Bellini and S. R. Zaki, *Emerging Infect. Dis.*, 2004, **10**, 320–326.
14 J. Zhai, S. Sarkar, C. E. Conn and C. J. Drummond, *Mol. Syst. Des. Eng.*, 2020, **5**, 1354–1375.

15 R. Negrini, A. Sánchez-Ferrer and R. Mezzenga, *Langmuir*, 2014, **30**, 4280–4288.
16 B. Fan, J. Wan, J. Zhai, X. Chen and S. H. Thang, *ACS Nano*, 2021, **15**, 16.
17 P. Nogly, D. James, D. Wang, T. A. White, N. Zatsepin, A. Shilova, G. Nelson, H. Liu, L. Johansson, M. Heymann, K. Jaeger, M. Metz, C. Wickstrand, W. Wu, P. Båth, P. Berntsen, D. Oberthuer, V. Panneels, V. Cherezov, H. Chapman, G. Schertler, R. Neutze, J. Spence, I. Moraes, M. Burghammer, J. Standfuss and U. Weierstall, *IUCrJ*, 2015, **2**, 168–176.
18 L. Van Dalsen, L. Smithers, C. Boland, D. Weichert and M. Caffrey, *Cryst. Growth Des.*, 2020, **21**, 500.
19 A. Angelova, B. Angelov, M. Drechsler, T. Bizien, Y. E. Gorshkova and Y. Deng, *Front. Cell Dev. Biol.*, 2021, 9.
20 J. J. Vallooran, M. Duss, P. Ansorge, R. Mezzenga and E. M. Landau, *Langmuir*, 2020, **36**, 9132–9141.
21 R. H. Templer, J. M. Seddon, N. A. Warrender, A. Syrykh, Z. Huang, R. Winter and J. Erbes, *J. Phys. Chem. B*, 1998, **102**, 7251–7261.
22 A. I. I. Tyler, H. M. G. Barriga, E. S. Parsons, N. L. C. McCarthy, O. Ces, R. V. Law, J. M. Seddon and N. J. Brooks, *Soft Matter*, 2015, **11**, 3279–3286.
23 M. C. G. Lotierzo, B. R. Casadei, R. D. de Castro, B. Malheiros and L. R. S. Barbosa, *Drug Delivery Transl. Res.*, 2020, **10**, 1571–1583.
24 S. Rajesh, J. Zhai, C. J. Drummond and N. Tran, *J. Colloid Interface Sci.*, 2021, **589**, 85–95.
25 H. M. G. Barriga, A. I. I. Tyler, N. L. C. McCarthy, E. S. Parsons, O. Ces, R. V. Law, J. M. Seddon and N. J. Brooks, *Soft Matter*, 2015, **11**, 600–607.
26 H. L. Kantor and J. H. Prestegard, *Biochemistry*, 1978, **17**, 3592–3597.
27 A. Angelova, B. Angelov, V. M. Garamus and M. Drechsler, *J. Mol. Liq.*, 2019, **279**, 518–523.
28 R. W. Ordway, J. J. Singer and J. V. Walsh, *Trends Neurosci.*, 1991, **14**, 96–100.
29 G. Maulucci, O. Cohen, B. Daniel, A. Sansone, P. I. Petropoulou, S. Filou, A. Spyridonidis, G. Pani, M. De Spirito, C. Chatgilialoglu, C. Ferreri, K. E. Kypreos and S. Sasson, *Free Radic. Res.*, 2016, **50**, S40–S50.
30 A. I. I. Tyler, J. L. Greenfield, J. M. Seddon, N. J. Brooks and S. Purushothaman, *Front. Cell Dev. Biol.*, 2019, **7**, 187.
31 M. Ibarguren, D. J. López and P. V. Escribá, *Biochim. Biophys. Acta, Biomembr.*, 1838, **2014**, 1518–1528.
32 S. Terés, G. Barceló-Coblijn, M. Benet, R. Álvarez, R. Bressani, J. E. Halver and P. V. Escribá, *Proc. Natl. Acad. Sci. U. S. A.*, 2008, **105**, 13811–13816.
33 G. Carta, E. Murru, S. Banni and C. Manca, *Front. Physiol.*, 2017, **8**, 902.
34 M. Ricchi, M. R. Odoardi, L. Carulli, C. Anzivino, S. Ballestri, A. Pinetti, L. I. Fantoni, F. Marra, M. Bertolotti, S. Banni, A. Lonardo, N. Carulli and P. Loria, *J. Gastroenterol. Hepatol.*, 2009, **24**, 830–840.
35 J. M. Seddon, R. H. Templer, N. A. Warrender, Z. Huang, G. Cevc and D. Marsh, *Biochim. Biophys. Acta, Biomembr.*, 1997, **1327**, 131–147.
36 S. Mabrey and J. M. Sturtevant, *Biochim. Biophys. Acta, Lipids Lipid Metab.*, 1977, **486**, 444–450.
37 D. Marsh and J. M. Seddon, *Biochim. Biophys. Acta, Biomembr.*, 1982, **690**, 117–123.
38 J. M. Seddon, A. M. Squires, C. E. Conn, O. Ces, A. J. Heron, X. Mulet, G. C. Shearman, R. H. Templer, H. F. Gleeson, V. Percec, S. T. Lagerwall, P. Palffy-Muhoray and C. R. Safinya, *Philos. Trans. R. Soc., A*, 2006, **364**, 2635–2655.
39 R. D. Koynova, B. G. Tenchovl, P. J. Quinn and P. Laggner, *Chem. Phys. Lipids*, 1988, **48**, 205–214.
40 R. D. Koynova, A. I. Boyanov and B. G. Tenchov, *Biochim. Biophys. Acta, Biomembr.*, 1987, **903**, 186–196.
41 A. Bouchet, F. Lairion and A. Disalvo, *Biochim. Biophys. Acta, Biomembr.*, 2012, **1818**, 1395–1401.
42 F. Hirata, J. F. Tallman, R. C. Henneberry, P. Mallorga, W. J. Strittmatter and J. Axelrod, *Prog. Clin. Biol. Res.*, 1981, **63**, 383–388.
43 J. M. Seddon, G. Cevc, R. D. Kaye and D. Marsh, *Biochemistry*, 1984, **23**, 2634–2644.
44 R. Koynova and B. Tenchov, *Data Br.*, 2018, **18**, 501–505.
45 S. M. Gruner, M. W. Tate, G. L. Kirk, P. T. C. So, D. C. Turner, D. T. Keane, C. P. S. Tilcock and P. R. Cullis, *Biochemistry*, 1988, **27**, 2853–2866.
46 M. Kusube, H. Matsuki and S. Kaneshina, *Biochim. Biophys. Acta, Biomembr.*, 1668, **2005**, 25–32.
47 M. Kusube, M. Goto, N. Tamai, H. Matsuki and S. Kaneshina, *Chem. Phys. Lipids*, 2006, **142**, 94–102.
48 D. P. Siegel and J. L. Banschbach, *Biochemistry*, 1990, **29**, 5975–5981.
49 V. Cherezov, D. P. Siegel, W. Shaw, S. W. Burgess and M. Caffrey, *J. Membr. Biol.*, 2003, **195**, 165–182.
50 G. L. Kirk, S. M. Gruner and D. L. Stein, *Biochemistry*, 1984, **23**, 1093–1102.
51 M. Fornasier, R. Pireddu, A. Del Giudice, C. Sinico, T. Nylander, K. Schillén, L. Galantini and S. Murgia, *Colloids Surf., B*, 2021, **199**, 111564.
52 B. R. Pauw, A. J. Smith, T. Snow, N. J. Terrill and A. F. Thünemann, *J. Appl. Crystallogr.*, 2017, **50**, 1800–1811.
53 R. Koynova, B. Tenchov and G. Rapp, *Chem. Phys. Lipids*, 1997, **88**, 45–61.
54 G. Pabst, N. Kučerka, M.-P. Nieh and J. Katsaras, *Liposomes, Lipid Bilayers and Model Membranes: From Basic Research to Application*, CRC Press, 2014.
55 R. H. Templer, J. M. Seddon and N. A. Warrender, *Biophys. Chem.*, 1994, **49**, 1–12.
56 D. P. Siegel, *Biophys. J.*, 1993, **65**, 2124–2140.
57 D. P. Siegel, *Biophys. J.*, 1999, **76**, 291–313.
58 D. P. Siegel and M. M. Kozlov, *Biophys. J.*, 2004, **87**, 366–374.
59 J. T. Mason and T. J. O'Leary, *Biophys. J.*, 1990, **58**, 277–281.
60 T. J. McIntosh, *Chem. Phys. Lipids*, 1996, **81**, 117–131.
61 P. M. Brown, J. Steers, S. W. Hui, P. L. Yeagle and J. R. Silvius, *Biochemistry*, 1986, **25**, 4259–4267.
62 H. L. Casal and H. H. Mantsch, *Biochim. Biophys. Acta, Biomembr.*, 1983, **735**, 387–396.
63 T. J. McIntosh and S. A. Simon, *Biochemistry*, 1986, **25**, 8474.
64 T. J. McIntosh, *Biophys. J.*, 1980, **29**, 237–245.